Environmental Pollution 295 (2022) 118696

Contents lists available at ScienceDirect

Environmental Pollution

journal homepage: www.elsevier.com/locate/envpol

Temporal variations of soil NO and NO_2 fluxes in two typical subtropical forests receiving contrasting rates of N deposition☆

Piaopiao Ke [a,1], Ronghua Kang [b,1], Loreena K. Avery [a], Jiawei Zhang [a], Qian Yu [a], Danni Xie [c], Lei Duan [a,*]

[a] State Key Laboratory of Environmental Simulation and Pollution Control, School of Environment, Tsinghua University, Beijing, 100084, China
[b] CAS Key Laboratory of Forest Ecology and Management, Institute of Applied Ecology, Chinese Academy of Sciences, Shenyang, 110016, China
[c] School of Land Engineering, Chang'an University, Shanxi, 710064, China

ARTICLE INFO

Keywords:
Subtropical forest
Soil emission
Nitrogen deposition
Nitrogen status
Nitrification

ABSTRACT

Soils have been widely acknowledged as important natural sources of nitric oxide (NO) and meanwhile sinks of nitric dioxide (NO_2). High nitrogen deposition across South China could potentially result in large NO emissions from subtropical forests soils there. In this study, the dynamic chamber method was applied to monitor NO and NO_2 fluxes at two subtropical forest sites in South China, namely "Qianyanzhou" (QYZ) and "Tieshanping" (TSP). Chronically higher N deposition occurred at TSP than that at QYZ. Besides soil water filled pore spaces (WFPS) and temperature, ambient NO concentration could also possibly be important in regulating temporal NO emissions, especially in the winter. For both sites, the optimum soil temperature was above 25 °C, while the optimum WFPS for NO release at QYZ was higher (65–70%) than that at TSP (<23%). Moreover, heavy rainfall could trigger NO emission pulses from moist soils at QYZ, while rainfall-induced NO pulses were only observed after a long drying period at TSP. Distinctly different contents of mineral nitrogen and soil moisture conditions between the two sites might induce the divergent preference of WFPS and responses to rainfall. The cumulative soil emission of NO reached 0.41 ± 0.01 and 0.76 ± 0.01 kg N ha^{-1} yr^{-1} at QYZ and TSP, contributing to 2.5% and 1.4% of the annual throughfall N input, respectively. At both sites, NO_2 were mainly deposited to soils, accounting for 2% and 21% of soil-emitted NO at QYZ and TSP, respectively. The observed annual NO emissions at these two sites were larger than the median values observed for tropical and temperate forests and unfertilized croplands. Higher N deposition could induce larger NO emission potential, while soil temperature and pH might also be important in regulating regional soil NO emissions as N-loss from subtropical forests.

1. Introduction

Nitrogen oxides (NO_x, representing the sum of NO and NO_2) are important air pollutants and play significant roles in atmospheric chemistry (Crutzen, 1979). The anthropogenically and naturally emitted NO could be quickly oxidized to NO_2 in the air (Seinfeld and Pandis, 2012) and eventually influence the atmospheric oxidative capacity (Altshuller and Bufalini, 1971), aerosol formation (Seinfeld and Pandis, 2012), and atmospheric N input into ecosystems (Galloway et al., 2004). Soils have been widely acknowledged as important natural sources of NO (Holland et al., 1999; Butterbach-Bahl et al., 2009), which contributed to approximately 40% of global NO_x emission in pre-industrial times (Holland et al., 1999) and 10–15% in recent decades (Weng et al., 2020; and the reference therein). NO in soils is mainly produced as intermediates of microbial denitrification and nitrification processes (Firestone and Davidson, 1989; Medinets et al., 2015), which are favored under anaerobic and aerobic conditions, respectively. These two processes can occur simultaneously within the same soil aggregates (Medinets et al., 2015). Additionally, it has been recently reported that NO is an obligate bacterial nitrification intermediate produced from hydroxylamine oxidation (Caranto and Lancaster, 2017). The abiotic decomposition of nitrite (NO_2^-) could be another important source of NO in acid soils (Udert et al., 2005; Homyak et al., 2017). Notably, NO released from soil is greatly lower than NO produced as soil could also

☆ This paper has been recommended for acceptance by Jörg Rinklebe.
* Corresponding author.
E-mail address: lduan@tsinghua.edu.cn (L. Duan).
[1] authors contributed equally.

https://doi.org/10.1016/j.envpol.2021.118696
Received 13 July 2021; Received in revised form 3 December 2021; Accepted 14 December 2021
Available online 22 December 2021

absorb and/or consume NO, such as during the denitrification process (Medinets et al., 2015; Medinets et al., 2019). Abiotic factors, e.g., soil moisture and temperature, are anticipated to regulate fluctuations of soil NO emissions (Pilegaard, 2013), while availability of nitrogen substrates (mainly NO_3^- and NH_4^+ for denitrification and nitrification process, respectively; Pilegaard, 2013) is likely to determine the magnitude of soil NO emission (Firestone and Davidson, 1989). Furthermore, NO_2, either from transfer of polluted air-mass or oxidation of soil-emitted NO, could be deposited to soil surfaces (ButterbachBahl et al., 1997; Gut et al., 2002) or uptake by plants (Ganzeveld et al., 2002), possibly affecting net NO_x flux from forests to atmosphere.

Despite its importance, global budget of soil NO emission is highly uncertain. The existing global inventory of soil NO emission has been reported in a wide range, from 4.8 to 21 Tg N yr^{-1} (Weng et al., 2020; and the reference therein), which calls for more field observations for accurate evaluation of the budget. Subtropical forests in South China (147 million ha; FAO, 2020) compose 33% of the global subtropical forests, where chronically high N deposition has been widely documented (Schwede et al., 2018; Yu et al., 2018). High nitrogen deposition could possibly trigger strong NO emission from soils (Pilegaard et al., 2006; Liu et al., 2017). However, to our knowledge, only three subtropical forest sites have been investigated for soil NO emissions (Li et al., 2007; Kang et al., 2017), and the response of soil NO emission in subtropical forests to atmospheric N deposition remains little understood. Furthermore, these studies in subtropical forests were only conducted either in the summer or in the daytime. Considering the large spatiotemporal variations of soil NO emission (Ganzeveld et al., 2002; Li et al., 2007; Kang et al., 2017), more long-term field investigations in subtropical forests are required to precisely evaluate contributions of soil NO emissions to total NO_x budget (Huang and Li, 2014) and regional air pollution, especially in rural areas (Lu et al., 2021).

In this study, NO and NO_2 fluxes were monitored over 6 months in two *Pinus massoniana* subtropical forests in South China, receiving contrasting rates of atmospheric N deposition. The objectives of this study were to: (1) investigate temporal variations of NO and NO_2 fluxes at the two sites and their controlling factors, (2) identify impacts of N deposition on soil NO emissions, and (3) estimate the budget of NO_x emission from these subtropical forests.

2. Methods

2.1. Site description

In this study, NO and NO_2 fluxes above soils were investigated at two typical *Pinus massoniana* forests in South China (Table 1), namely "Qianyanzhou" (QYZ) and "Tieshanping" (TSP). QYZ is located 42 km southwest to Ji'an city center (Jiangxi Province, China), managed by the Chinese Academy of Sciences (CAS). This site is surrounded by forests within area of ca. 17 ha. TSP, located 25 km northeast to the center of Chongqing city, is a secondary forest of around 16 ha. The inorganic N deposition and soil extractable NH_4^+ at TSP were ~2-fold of those at QYZ (Table 1). Typically, rainfall events concentrate during April to September at both sites, inducing humid summer and relatively dry winter. These areas are also subjected to episodic drought events in summer time (Wen et al., 2010). During the investigation, the summer was humid with total rainfall of 457 mm at QYZ, while month-long drought with no rainfall events in August (total rainfall being 273 mm in the summer) occurred at TSP.

2.2. Measurement of NO and NO_2 concentrations and fluxes

The NO and NO_2 flux measurements were conducted during June–November 2018 at QYZ and May 2020–April 2021 at TSP. At both sites, the NO and NO_2 fluxes were continuously measured for 6 days every month with the dynamic chamber method (Figure S1), using two 16 L opaque PVC chambers (400 × 400 mm with height of 100 mm; Kang et al., 2017). The soil chamber was open at the bottom, allowing exchanges between soils and air, while the reference chamber was closed at the bottom. The backside of the two chambers had evenly distributed circular air inlets to ensure even and stable flow of ambient air inside the chambers (Figure S1). An external pump was utilized to accelerate the flow in the chamber at a rate of 8 L min^{-1}. The measurement of concentrations in the two chambers was switched every 10 min and continuously operated over the whole day. Considering possible NO accumulation in the chamber at the beginning of every switch, data of the first 4 min in each run (plenty for evacuating the chamber) were discarded in the flux calculation. The NO and NO_2 concentrations were sequentially measured inside a commercial NO_x analyzer (Model 42i-TL Thermo Environmental Instruments, USA; detection limit: 0.05 ppbv, zero noise: 0.025 ppb) on a 10-s cycle. The NO_2 was converted to NO at 325 °C by a molybdenum inside the analyzer and then measured through the chemiluminescent reaction between NO and O_3. Other reactive oxidized nitrogen species, e.g., nitrous acid (HONO) and nitric acid (HNO_3), could possibly interfere with the thermal conversion of NO_2 (Kleffmann et al., 2013). However, the interference in rural environments could possibly be minor, as monitored HONO concentration was 5–7% of NO_2 concentration in rural area (Li et al., 2012; Sörgel et al., 2015), and effective thermal dissociation of HONO is often 640 °C (Perez et al., 2007). The NO_x analyzer was calibrated before each measurement in the month with NO concentrations between 5 and 50 ppb diluted from 10-ppm standard NO in N_2 with zeroed air (air filtered by active alumina covered with potassium permanganate and then active carbon) by a gas mixer (Beijing Seven-star Electronics Co. China; Kang et al., 2017). At each site, three plots with little or no herb covering were chosen for the measurement (approximately 4 m away from each other) without disturbing the aboveground biomass. During each monitoring period, the two chambers were moved every day from one plot to another clockwise to prevent influences of the chamber covering to soil properties underneath.

The fluxes calculation (Section S1) was accordant with Kang et al. (2017). Since NO_2 fluxes were comparable and negligible to NO fluxes after chemical conversion in the monitoring systems at TSP and QYZ, respectively (Figure S2), the NO and NO_2 concentrations correction was

Table 1
Characteristics of the two subtropical forest sites. All soil data are presented for layer of 0–10 cm depth measured in the end of growth season.

Site	QYZ	TSP
Location	115°4′E, 26°45′N	106°42′E, 29°37′N
Climate	Subtropical monsoon climate	
Mean annual temperature (°C)	19.2 [a]	17.0 [b]
Mean annual Precipitation (mm)	1494 [a]	1028 [b]
Soil type	Udic Ferrisols	Haplic Acrisol
Soil extractable NH_4^+ (mg N kg^{-1} wet soil)	5.11 [c]	10.0 [d]
Soil extractable NO_3^- (mg N kg^{-1} wet soil)	1.12 [c]	1.10 [d]
Soil pH	4.67 [c]	3.87 [e]
Soil C/N	17.2 [c]	20.6 [e]
Soil organic carbon (g kg^{-1})	13.4 [f]	21.7 [d]
Soil total nitrogen (g kg^{-1})	1.20 [f]	1.77 [d]
Soil texture	68% of silt and 15% of clay [g]	55% of silt and 27% of clay [h]
Basal area (cm^2 m^{-2})	0.33 [f]	0.18 [b]
Predominant plant type	*Pinus massoniana*	
Annual throughfall deposition of inorganic N (kg N ha^{-1} yr^{-1})	15.4	45.0

[a] Xu et al. (2011).
[b] Huang et al. (2015).
[c] Wang et al. (2019).
[d] Xie (2020).
[e] Zhu et al. (2013).
[f] Wang et al. (2015).
[g] Wen et al. (2010).
[h] Sørbotten (2011).

only made for TSP site (Section S1) according to ButterbachBahl et al. (1997) and Mayer et al. (2011). Furthermore, air pollution from the nearby city induced high concentrations of NO_x at TSP. The sudden and inconstant rises in NO and NO_2 concentrations could lead to errors in fluxes calculation when using the dynamic chamber method (Gut et al., 2002). In this study, if the changes of NO or NO_2 concentrations during the 10-min measurement of ambient concentration was larger than 2 ppbv, the flux data were excluded during the data processing. Additionally, gap-filling based on the empirical formulations have been verified to be helpful in improving the estimations of annual NO emissions (Li et al., 2007; Wu et al., 2010). In this study, an empirical fitting between NO flux, soil moisture and soil temperature was conducted for both sites, assuming that the emission rate was exponentially related to soil temperature (Medinets et al., 2015) and in quadratic relation to soil moisture (Li et al., 2007). All descriptive analysis and graph drawing were conducted in OriginPro 2021. The corrections of NO and NO_2 concentration and curve fittings were conducted in MATLAB 2019a.

2.3. Auxiliary measurement

The throughfall deposition of dissolved inorganic nitrogen (including NH_4^+ and NO_3^-) and the corresponding ion concentration and fluxes in the soil water (0–10 cm) were simultaneously monitored in two and three plots at QYZ and TSP, respectively (see detailed method in Yu et al., 2018). In addition, the total solar radiation, air temperature and relatively humidity were measured with weather stations above the forest canopies, while the soil temperature and volumetric water content were measure at 5 cm depth in soil at both sites (see Ke et al., 2020 for detailed sensor specification). Since water filled pore space (WFPS) could represent the soil moisture over different soil textures, WFPS was calculated at both sites according to Kang et al. (2017), with soil bulk density being 1.42 and 1.21 g cm^{-3} at QYZ (Wang et al., 2015) and TSP (Sørbotten, 2011), respectively. It should be noted that the top of the chamber was closed during the measurement, which blocked rainfall directly into the plots. As metal frames for chamber installation were ~3 cm deep under the soil, only rainfall that influenced soil moisture (indicated by WFPS) at 5 cm deep were considered in this study to investigate the effect of rainfall to soil NO emission. There might be delays and reductions of WFPS changes for soils covered by the chamber, leading to uncertainties in the investigations during rainfall events. However, as the monitoring for one plot continued for ~24 h, it shall be enough to observe rainfall effects (if existing) (Leitner et al., 2017; Barrat et al., 2020).

3. Results

3.1. Temporal patterns of NO and NO_2 concentrations and fluxes and their responses to rainfall in subtropical forests

At both sites, the ambient NO concentrations near the soil surfaces and soil NO emission fluxes were considerably higher during warmer seasons than those in the colder seasons (Table S1, Figs. 1 and 2), except for November at QYZ and September at TSP when rainfall events occurred. Near the ground floor (at 0–10 cm), the ambient NO_2 concentration was comparable to NO concentration at TSP, while it was much lower than NO concentration at QYZ. The ambient concentrations of NO and NO_2 at the forest floor were significantly larger at TSP than those at QYZ ($P < 0.05$). The NO flux ranged from −1.31 to 85.4 (11.5 ± 0.6, mean ± standard error) μg N m^{-2} h^{-1} at QYZ, and from −21.7 to 326 (8.16 ± 0.55) μg N m^{-2} h^{-1} at TSP. Stronger NO emission was accompanied with higher NO concentration at QYZ., e.g., significantly higher NO concentration and NO flux on July 19th than the three days before ($P < 0.05$; Fig. 1). At TSP, the net NO flux was negative (deposited or consumed by the soils) in the winter when the ambient NO concentration rapidly increased (Fig. 2). The daily maximum NO emission was often observed at night (between 19:00 and 6:00) at QYZ, while at TSP, the maximum NO emission was observed in the day (between 11:00 and 18:00) if NO-polluted air mass was not transferred to and detected at this site, i.e., inconstantly increased NO concentration. Compared to the NO flux, NO_2 flux was generally negligible (absolute values < 5 μg N m^{-2} h^{-1}) at both sites except in November at QYZ or in May, August, September and winter months at TSP. Both depositions and periodic emissions of NO_2 appeared at the two sites. The diurnal cycle of NO_2 was not distinct, especially in the winter at TSP, when the fluctuations of NO_2 flux primarily followed variations of ambient NO_2 concentration ($r = -0.79$, $P < 0.05$; Figure S3). Furthermore, the NO_2 flux insignificantly correlated with the NO flux at QYZ ($P > 0.1$), while a strong negative correlation occurred at TSP ($r = -0.66$, $P < 0.05$; Table S3), apart from winter periods when depositions of both gases were detected.

During the monitoring, rainfall episodes occurred and induced

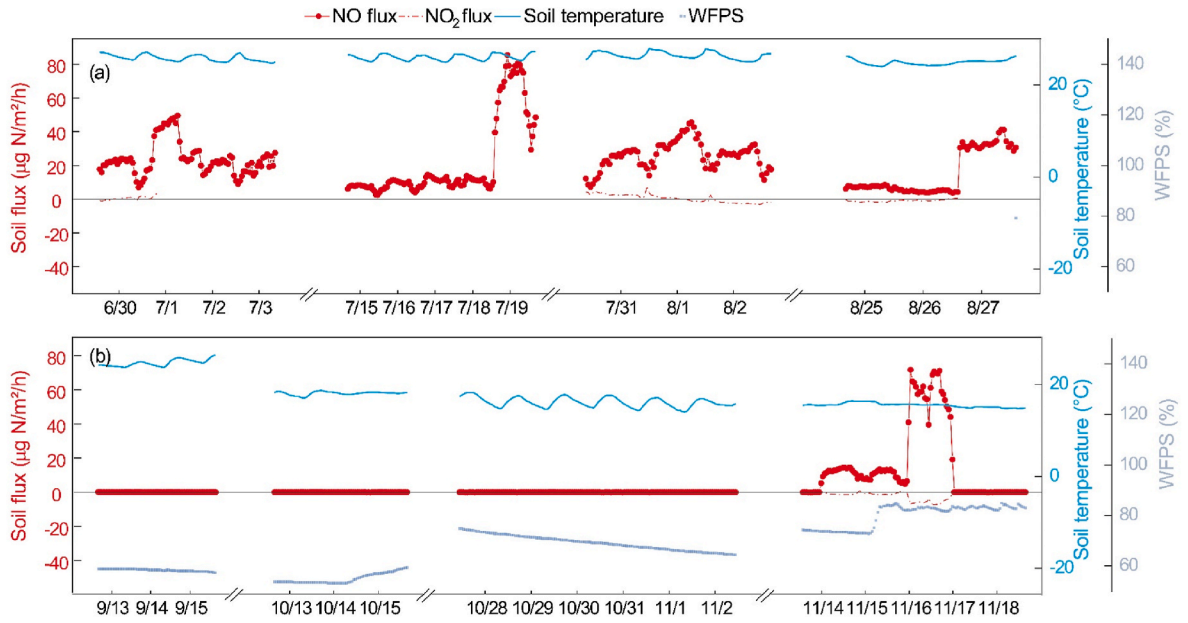

Fig. 1. The hourly variation of NO and NO_2 fluxes at QYZ along with soil temperature and WFPS in the summer (a) and autumn (b). The time of all the labelled date was 00:00. X-axis scales are different for various seasons.

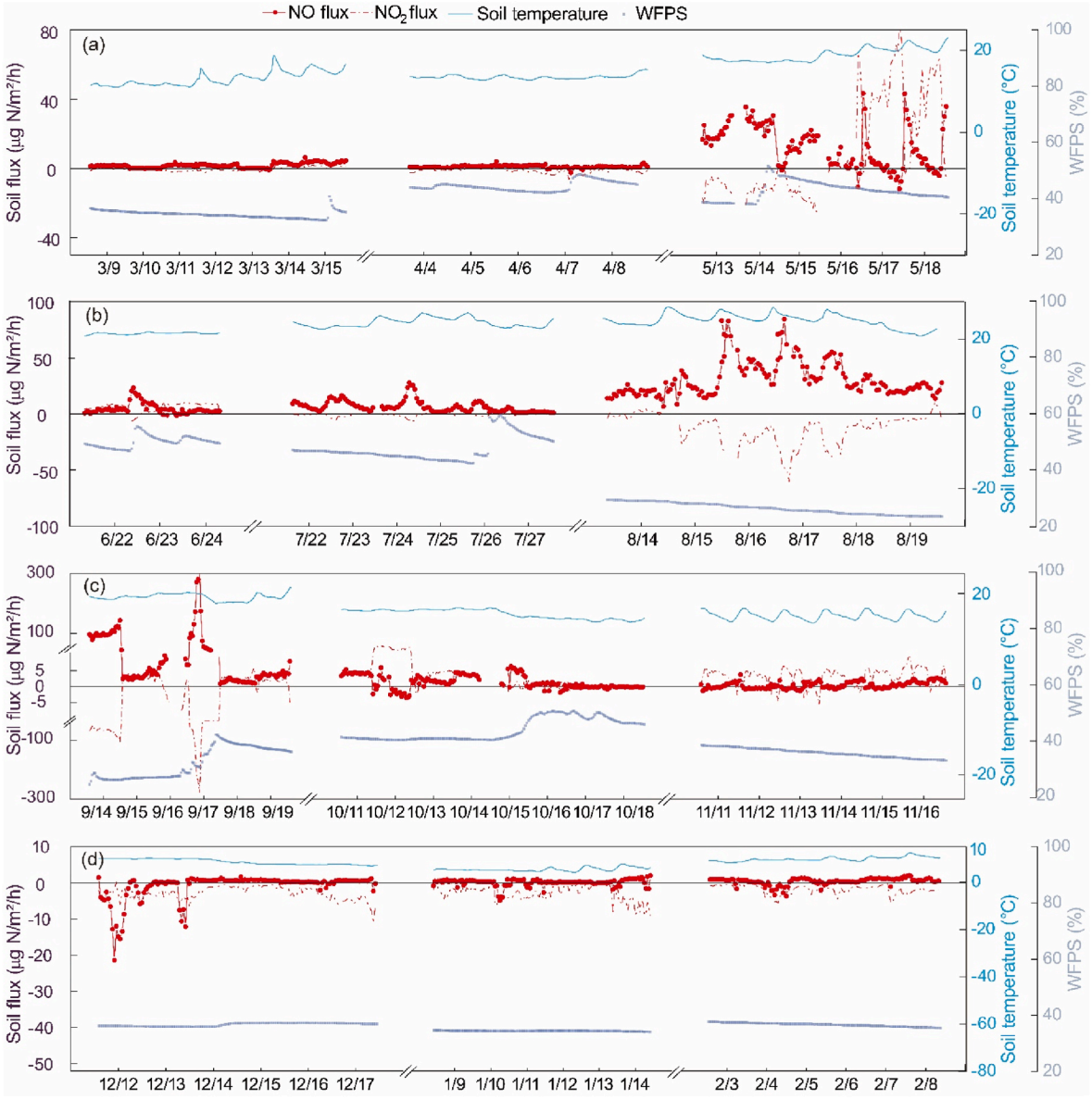

Fig. 2. The hourly variation of NO and NO_2 flux at TSP along with soil temperature and WFPS in the spring (a), summer (b), autumn (c) and winter (d). The time of all the labelled date was 00:00. X-axis scales are different for various seasons.

different responses at QYZ and TSP (Table 2). Strong NO pulses were observed at QYZ as long as the rainfalls were heavy (>27 mm day^{-1} in this study), with possibly high nitrogen deposition (>0.27 kg N ha^{-1} day^{-1}), even in the November when the soil was wet and relatively cold. The highest NO pulse reached up to 71.7 μg N m^{-2} h^{-1}, leading to 52% increase of mean hourly NO emission during the 4 h since rainfall started (detected by WFPS change), in comparison with that over the 4 h prior to the rain (Table 2). In contrast, the rainfall event at TSP induced distinctly higher NO emissions only after a long drying period (>30 days). The NO pulse peaked 2.1 times of the flux before the rain, surpassing 300 μg N m^{-2} h^{-1}, while in other seasons, the rainfall inhibited the soil NO emission, amounting to 72% reduction (Table 2).

3.2. Effects of WFPS, soil temperature and ambient NO concentration on soil NO emission

Soil moisture and temperature were the dominant environment factors influencing the NO emissions at both sites (Table S2 and S3). Soil moisture was significantly negatively correlated with NO flux ($r = -0.27$ for QYZ and -0.18 for TSP, $P < 0.05$), while soil temperature was positively correlated with NO flux at both sites ($r = 0.62$ for QYZ and 0.55 for TSP, $P < 0.05$), except in the winter period at TSP. High emissions of NO clustered with soil temperature higher than 25 °C at both sites (Fig. 3). The soil at QYZ showed an optimum WFPS between 65% and 70%, while the NO emission continuously increased with declined soil water content and the optimum WFPS was less than 23% at TSP. In addition to WFPS and soil temperature, high ambient NO concentration at TSP (>20 ppbv) led to significant deposition in the winter (soil temperature <10 °C), and significantly inhibited net NO release from soils in other seasons ($r = -0.21$, $P < 0.05$; Figure S4). Nevertheless, at QYZ, the NO flux was positively associated with ambient NO concentration in both the summer and autumn ($r = 0.86$, $P < 0.01$; Figure S4).

Based on the correlation among NO flux, WFPS, and soil temperature, empirical regression analysis was conducted at both sites. At QYZ, the empirical formulation was as follows ($n = 852$, $P < 0.05$ $R^2 = 0.42$):

$$F_{NO} = \left(-2.35 \times 10^{-4}(\mathrm{WFPS} - 64.9)^2 + 0.0775\right) \times e^{0.210T} \quad (2)$$

Table 2
Impacts of rainfall (indicated by WFPS change) on NO fluxes at QYZ and TSP (Data format: averaged values during the 4 h before rainfall started and the relative changes in the 4 h immediately after the rainfall started. Positive values indicated enhancement effect, and vice versa).

Date	Rainfall (mm day^{-1}) [a]	TF [b] (kg N ha^{-1} d^{-1})	NO flux (μg N m^{-2} h^{-1})	NO concentration (ppb)	Antecedent drying days (d)	Soil WFPS (%)	Soil temperature (°C)
QYZ							
7/2	93	1.36	16.5 (+22%)	7.0 (+35%)	11.0	59.1 (+6%)	26.4 (−4%)
8/25	27	0.27	4.6 (−12%)	1.8 (−2%)	2.8	65.4 (+8%)	24.5 (−0.8%)
8/26	27	0.27	31.1 (+2%)	19.7 (+2%)	0.5	74.0 (+1%)	25.1 (+0.4%)
10/14	13	0.18	—— [c]	0.06	3.7	52.8 (+1%)	17.9 (−0.2%)
11/15	55	0.44	7.7 (+52%)	4.2 (−6%)	2.2	71.8 (+7%)	16.3 (−2%)
TSP							
3/15	6	0.24	3.7 (−38%)	1.2 (+18%)	7.1	37.9 (+19%)	15.2 (+5%)
4/7	23	1.31	0.7 (−1.5)	0.2 (13)	6.1	49.9 (+8%)	13.0 (+0.2%)
5/13	23	0.80	29.1 (-13%)	4.5 (+27%)	2.5	44.3 (+8%)	17.4 (−1%)
7/26	61	1.03	8.2 (−72%)	7.8 (−80%)	8.5	52.8 (+28%)	24.7 (−0.4%)
9/16 [d]	90	1.23	90.1 (+110%)	1.7 (+30%)	34.5	28.5 (+13%)	19.7 (+5%)
10/15	3	0.02	0.9 (−55%)	0.7 (+6)	8.0	57.0 (+1%)	15.4 (−0.7%)

[a] Estimated as weekly accumulated rainfall divided by frequency of rainfall event in the week including the day.
[b] Throughfall deposition of inorganic nitrogen during the rainfall event.
[c] Below the detection limit.
[d] Comparison made over different days at the same plot.

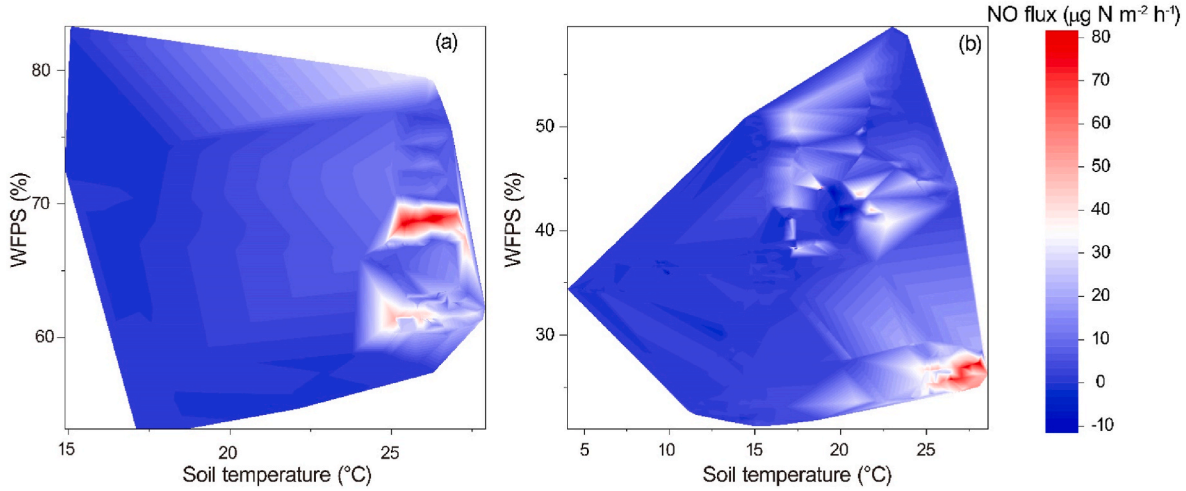

Fig. 3. The variation of hourly NO flux with soil temperature and soil water content at QYZ (a) and TSP (b). Data impacted by rainfall, i.e., continuously increased WFPS, were excluded in the graph.

where WFPS and T were the water filled pore space (%) and soil temperature (°C), respectively. Moreover, insignificant emissions of NO were observed with low WFPS at QYZ site (Fig. 1). Hence, hourly fluxes with WFPS below 58% were estimated to be zero in the simulation.

At TSP, an optimum WFPS was not observed in this study and fixed to at 21%, equal to observations from previous incubation studies (Kang, unpublished data). Considering the significant NO consumption due to high ambient concentrations in the winter at TSP (soil temperature <10 °C; Figure S4), the simulation of NO fluxes was divided into two stages as warm condition (soil temperature >10 °C, $n = 1237$, $P < 0.05$, $R^2 = 0.28$) and cold condition (soil temperature <10 °C, $n = 370$, $P <$

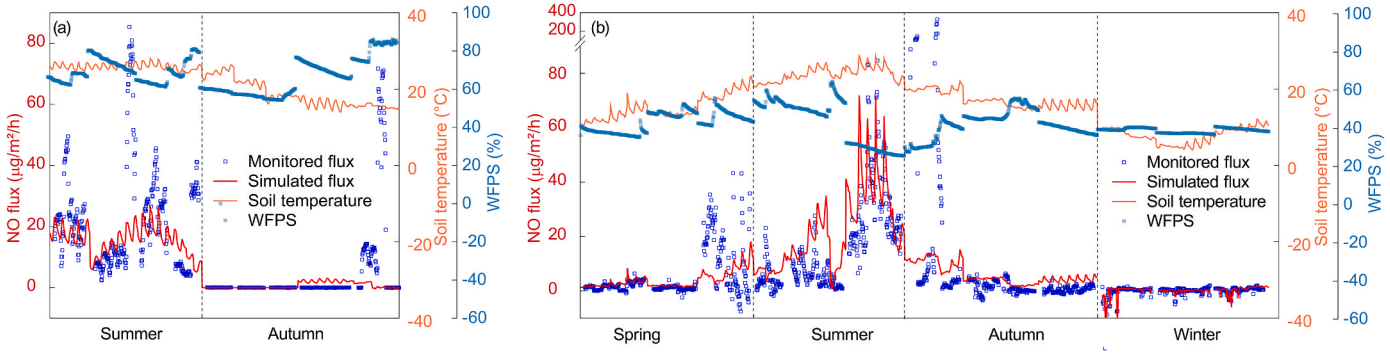

Fig. 4. The simulation results of NO flux at QYZ (a) and TSP (b) based on equations (2) and (3) and (4), respectively.

0.05, $R^2 = 0.92$):

$$F_{NO} = \left(-0.939 \times 10^{-5}(\mathrm{WFPS} - 21.0)^2 + 0.180 \right) \times e^{0.210T},\ T > 10^{\circ}C \quad (3)$$

$$F_{NO} = (-0.0517 c_{NO} + 0.131) \times e^{0.210T},\ T < 10^{\circ}C \quad (4)$$

where c_{NO} was the ambient NO concentration.

The simulations above were unable to predict the pulsing effect (Fig. 4), such as in November at QYZ and September at TSP; they did, however, fitted well with the seasonal variations of NO fluxes. If excluding flux data influenced by rainfall, the coefficients of determination of above simulations could be as large as 0.62 and 0.60 at QYZ and TSP, respectively.

4. Discussion

4.1. Factors controlling NO fluxes from subtropical forest soils: on site scale

The controlling of soil WFPS and temperature on soil NO emissions coincided with numerous laboratory incubations studies (e.g., Yu et al., 2008; Bargsten et al., 2010; Yu et al., 2010) and field investigations over various ecosystems (e.g., ButterbachBahl et al., 1997; Butterbach-Bahl et al., 2004; Pilegaard et al., 2006; Kang et al., 2017). Li et al. (2007) also observed this in a broadleaf forest and a *Pinus massoniana* forest (DHS site) in Southeast China. It is suggested that WFPS is tightly connected with soil NO emission through regulating gas and substrate diffusivity (Schindlbacher et al., 2004; Pilegaard, 2013), oxygen supply (Medinets et al., 2015), and thus influencing activities of functional microbial groups involved in NO production (Behrendt et al., 2017). According to an isotope tracing experiment (Kang et al., 2019) at TSP site, nitrification, primarily autotrophic nitrification, was the major process contributing to NO emission when WFPS was below 60%. Notably, WFPS at QYZ was significantly larger than that at TSP ($P < 0.05$), although the water holding capacity could possibly be larger at TSP than that at QYZ due to larger contents of organic matter and clay at TSP (Table 1; Li et al., 2007). TSP site was sloping (6–13%), while QYZ was relatively flat. The flatter topography, more frequent rainfall and denser plant coverage at QYZ (Table 1) all possibly induced higher soil WFPS than that at TSP. In the laboratory incubation of soil cores collected at TSP (Kang, unpublished data), the optimum WFPS for NO emission was 21%, which coincided with the results in this study. Contrastively, at QYZ, when low WFPS occurred in the autumn (correlated with reduced precipitation and thus limited atmospheric N input), the NO emission became insignificant (Fig. 3). Particularly, the soil extractable NH_4^+ at TSP was approximately 2-fold of those at QYZ (Table 1), possibly due to chronically high N deposition at TSP (Huang et al., 2015). Hence, it is reasonable to hypothesize that more abundant mineral N (sum of extractable NO_3^- and NH_4^+) might result in preference of lower WFPS at TSP than at QYZ as more aerobic conditions favor NO production from nitrification process if substrate is not limited (Bargsten et al., 2010). In the case of QYZ, soil NO emissions might depend more on the substrate diffusion in soils and atmospheric N input from precipitations (Section 4.2) than those at TSP, i.e., relying on higher soil WFPS. Furthermore, at QYZ, WFPS could reach more than 60% (Fig. 1), where nitrifier denitrification or identification process could possibly also contribute to soil NO emission (Pilegaard, 2013; Tian et al., 2019).

For both studied forests, the highest NO emissions were detected at soil temperature above 25 °C (Fig. 3), which was in the range of previously reported temperature optimums (22–30 °C) for nitrification but lower than the optimums (35 °C) detected in some tropical forests (Medinets et al., 2015; and the reference therein). The dependence of soil NO emission on soil temperature could result in largely declined production rates of NO in the winter (soil temperature below 10 °C; Bargsten et al., 2010). Moreover, in the winter at TSP, significant depositions of NO occurred instead of emissions. It is well acknowledged that observed NO fluxes above soils are results of NO productions counteracted by the consumptions (Bargsten et al., 2010; Behrendt et al., 2014), which occurs simultaneously in soil and the NO consumption rate is proportional to the ambient NO concentration (Bargsten et al., 2010). At TSP site, net NO consumption occurred with WFPS <40% and soil temperature <10 °C when the ambient NO concentration was higher than 10 ppbv (Fig. 2), while the soil remained as a net NO source with WFPS <60% and soil temperature at 30 °C when ambient NO concentration was 300 ppbv (Kang, unpublished data). As reported for temperate forest soils (Bargsten et al., 2010; Behrendt et al., 2014), production rates of NO decreased much faster with soil temperature than that of consumption rate, which might explain the significant consumption of NO at TSP in the winter.

4.2. Different response to the rainfall events: influences of N availability on NO emissions

NO emission pulses triggered by rainfall events were observed for both sites, which were generally observed after a long drying period over various ecosystems (Davidson et al., 1991; Butterbach-Bahl et al., 2004; Goldberg and Gebauer, 2009; Medinets et al., 2016a; Delon et al., 2017; Homyak et al., 2017; Leitner et al., 2017; Pacifico et al., 2019; Song et al., 2020), including the other two subtropical forests in Southeast China (Li et al., 2007). NO emission from Australian tropical forest soils distinctly increased after the rainfall in the end of the dry season, whereby the NO pulses reached 500 μg N m^{-2} h^{-1}. However, the rainfall in wet seasons (WFPS >25%) no longer induced NO pulses (Butterbach-Bahl et al., 2004), which was similar to the case at TSP. During the drying process, the mineral and organic N are hypothesized to accumulate in soils due to reduced plant N uptake and hydrological disconnection between the microsites where mineralization and immobilization occur (Homyak et al., 2016; Leitner et al., 2017). Meanwhile, the biomass of the drought-resistant microbes could increase without implying an increase of their activity (Homyak et al., 2017; and the reference therein). Upon wetting of dry soils, faster diffusion of N substrates in the soil solution, an increased N supply from rainfall, and activation of microbes could all contribute to large NO pulses (Leitner et al., 2017). Additionally, microbial groups involved in NO production and consumption might hold different recovery rates from drought, leading to the accumulation of NO_2^- during wetting, and subsequently inducing NO emissions accompanied by chemodenitrification of NO_2^- (Heil et al., 2016).

In contrast to TSP, NO pulses due to rainfall events were still observed from moist soil (Table 2; WFPS >70%) at QYZ, although the magnitude of NO pulses was distinctly smaller than that at TSP (Table 2). NO pulses due to wetting of moist soils (WFPS >80% before wetting) have also been reported but after 18 days of drought by Medinets et al. (2021). In moist soil, mineral and organic N, and soil biomass are unlikely to accumulate as that during the drought (Homyak et al., 2017). The major impacts of rainfall on moist soil could be additional inorganic N input, increasing WFPS and influencing the state of the microbial community (Tian et al., 2019; Barrat et al., 2020). During heavy rainfall, excess N deposition (Butterbach-Bahl et al., 2004), together with disturbances in soil aggregates (Barrat et al., 2020), could induce a sudden flush of mineral N and carbon to soil microorganisms and then enhance NO production (Medinets et al., 2021). Moreover, Behrendt et al. (2017) observed optimal soil moisture under both dry and wet conditions in dryland and paddy soils, possibly caused by compositions of microbial community varying with soil moisture. As described above, at QYZ, nitrifier denitrification or denitrification process might also contribute to soil NO emissions under anaerobic conditions (Pilegaard, 2013). In conclusion, additional N supply, and possible contributions of denitrification process due to the heavy rainfall, might lead to the NO pulse in moist soils at QYZ. Nevertheless, the ample N content at TSP, comparing with QYZ, might result in insensitive responses of the microorganisms to additional nutrient supply induced by

heavy rainfall. The effects of rainfall to soil NO emission are hard to predict (Barrat et al., 2020), and great differences have been shown between the two forests in this study. The underlying mechanism for the different responses to rainfall and contributions of NO pulses to total soil NO emission requires further investigation.

4.3. Bi-directional NO_2 fluxes on forest floors

In this study, NO_2 fluxes were observed to be bi-directional, i.e., both deposition and emission were observed. In general, the two subtropical forest floors both acted as small sinks of NO_2, with the mean values of -0.27 ± 0.61 and -1.61 ± 0.47 μg N m^{-2} h^{-1} at QYZ and TSP, respectively. The deposited NO_2 accounted for 2% and 21% of soil-emitted NO at QYZ and TSP, respectively. Generally, soils are considered as sinks of NO_2 with the deposition flux proportional to the ambient concentration (Gut et al., 2002; Schindlbacher et al., 2004). This was the case for TSP (Figure S5) in the winter and the corresponding deposition velocity was 0.67 mm s^{-1}, in the upper range of that observed over rice fields (0.17–0.67 mm s^{-1}; Fang & Mu, 2009), and smaller than that on the tropical forest floor (2.51–2.78 mm s^{-1}; Gut et al., 2002). However, in warmer seasons, the linear correlation between NO_2 flux and concentration became weak. Moreover, at TSP, direct soil emissions of NO_2 were observed during the drying process of rainfall-induced wet soil with low ambient NO_2 concentration (<10 ppbv) and high soil temperature (>18 °C), and were positively correlated with relative humidity (Table S4). The positive emission rates of NO_2 ranged 0–82.4 μg N m^{-2} h^{-1}, ~2-fold of NO emission rates during the same monitoring time-points, and composed 35% of the monitoring period. The periodic NO_2 emissions from soil have also been reported over farmlands (0–200 μg N m^{-2} h^{-1}; Fang and Mu, 2009; Medinets et al., 2016a; Recio et al., 2020; Tang et al., 2020) and temperate forests (0–50 μg N m^{-2} h^{-1}; ButterbachBahl et al., 1997) in field investigations. The mechanism of NO_2 production from soils remains unknown so far (Recio et al., 2020; Tang et al., 2020). At QYZ, the observed NO_2 emission was positively related to total solar radiation and soil temperature (Table S4), possibly caused by stronger O_3 oxidation in the monitoring system in sunny days (Fang & Mu, 2009). At TSP, the NO_2 flux was corrected and irrelevant with oxidation by O_3 in the pipelines and chamber. In this study, NO_2 concertation was detected through a molybdenum NO_2-to-NO converter at 325 °C, which could also possibly convert part of HONO to NO and then detected as NO_2 (Kleffmann et al., 2013), especially under conditions favoring soil HONO emissions (Medinets et al., 2016a). As reported by Mushinski et al. (2019) and Wu et al. (2019), peak emissions of HONO from incubated soils were 1.2–5.4 times of NO emission peaks during wet-dry transition of soils, while one field investigation on arable lands showed that the mean soil HONO emission was only 20% of NO emission during 10 days' monitoring (Tang et al., 2020). The high temperature and wet conditions of soil might benefit soil HONO emission due to decreased HONO solubility in soil solutions and stimulated nitrate reduction (Wu et al., 2019). At TSP, deposition of NO_2 and interference of HONO emission could possibly be counteracted, even leading to the observed emissions of NO_2 (Recio et al., 2020) when ambient NO_2 concentration was low and the soil was humid and warm. It has also been suggested that NO_2 is produced from NO oxidation by O_2 on the soil surface (Mushinski et al., 2019). Moreover, NO_2 could be released during the decomposition of HONO, stimulated by low soil pH (Heil et al., 2016). Validations of mechanisms for observed NO_2 emissions calls for simultaneous investigations of NO, NO_2 and HONO fluxes above subtropical forest soils.

4.4. Contribution of soil NO_x emission from subtropical forests to the atmosphere

Based on the empirical regression in Section 3.2 (inputs being minutely measured soil moisture and temperature through the year and monthly averaged NO concentration), the annual soil emissions of NO were estimated at 0.41 ± 0.01 and 0.76 ± 0.01 kg N ha^{-1} yr^{-1} at QYZ and TSP (Figure S6), contributing to 2.6% and 1.7% of the annual throughfall N input, respectively. The inability to estimate pulses events, however, led to underestimation of soil NO emission in the autumn at TSP and in the spring and summer at QYZ when the rainfall events frequently occurred. The cumulative NO emission rates at QYZ and TSP were much smaller than that in another *Pinus massoniana* subtropical forest in China, DHS site (4.3 kg N ha^{-1} yr^{-1}; Li et al., 2007), but larger than the median values observed for tropical forests (0.34 kg N ha^{-1} yr^{-1}; Table S5; Hassler et al., 2017; Liu et al., 2017), temperate forests (0.18 kg N ha^{-1} yr^{-1}; Luo et al., 2012; Medinets et al., 2016b; Li et al., 2017; Liu et al., 2017; Molina-Herrera et al., 2017), temperate grasslands (0.19 kg N ha^{-1} yr^{-1}; Liu et al., 2017; Molina-Herrera et al., 2017), and unfertilized temperate (0.04 kg N ha^{-1} yr^{-1}; Medinets et al., 2016a; Liu et al., 2017; Recio et al., 2019), and subtropical cropland (0.11 kg N ha^{-1} yr^{-1}; Liu et al., 2017; Pacifico et al., 2019). This could possibly result from generally higher N deposition across subtropical zones in China (Schwede et al., 2018; Yu et al., 2018). However, for temperate coniferous forests receiving comparable N deposition with the two studied sites, NO emission rates were distinctly higher, reaching 6–8 kg N ha^{-1} yr^{-1} (Figure S7; Pilegaard et al., 2006). If extrapolating the average emission rate for the reported four subtropical forests so far to the rest all subtropical forests in China, a total NO emission of 0.45 Tg N yr^{-1} from the forest area in South China could be derived, and account for 5.2% of the global estimation of soil NO emission (Hudman et al., 2012). Notably, soils in *Pinus massoniana* forests are mainly associated with ectomycorrhizal fungi (Wang et al., 2013), while stands dominated by arbuscular mycorrhizal fungi tend to have greater N transformation rates and NO emission rates than ectomycorrhizal trees (Mushinski et al., 2019; Mushinski et al., 2021). In this study, the estimated soil NO emission for whole subtropical forest soils could possibly be underestimated as the estimation was majorly based on investigations on *Pinus massoniana* forests. More precise assessment of soil NO emissions from subtropical forests requires investigations in other types of forests, e.g., stands dominated by arbuscular mycorrhizal fungi.

Also, NO emission from temperate coniferous forests responded sensitively to atmospheric N inputs (Pilegaard et al., 2006), while the correlation between N deposition and NO emission was weak in *Pinus massoniana* dominated subtropical forests (Figure S7). The contribution of soil NO emission as N-loss to the total throughfall deposition at TSP was lowest among the three coniferous sites (Figure S7). Soil mineral N at the three sites occurred in the order: TSP > DHS > QYZ, and the soil pH followed the order: TSP < DHS < QYZ. In subtropical forests, the soil with more abundant mineral N showed larger emission potential, e.g., the maximum hourly emission rate occurred at TSP, peaking at 326 μg N m^{-2} h^{-1}. This was reasonable as N availability determines the magnitude of soil NO emission (Firestone and Davidson, 1989; Pilegaard, 2013). Nevertheless, the mean emission rate was largest at DHS (Figure S8), even though lower soil WFPS and abundant substrate at TSP should favor NO emissions (Pilegaard, 2013; Medinets et al., 2016a). The lowest soil temperature and pH at TSP may inhibit nitrification (Medinets et al., 2015), even though mineral N in soils was the largest among the three sites. Also, chemodenitrification, positively related with soil acidity temperature, might effectively regulate soil NO emission in acid forest soils (Heil et al., 2016). The lowest pH at TSP did not seemed to trigger overriding NO emissions from chemodenitrification. As chemodenitrification requires higher activation energies than nitrification and denitrification processes (Schindlbacher et al., 2004), dependence of chemodenitrification on soil temperature could also be stronger, which possibly suppressed chemodenitrification process at TSP due to the lowest soil temperature. Specific differentiation of nitrification, denitrification and chemodenitrification in regulating soil NO emission in subtropical forests requires more detailed investigations, e.g., applying isotope tracing experiment (Kang et al., 2019).

Moreover, soil emitted NO_x (the sum of simulated soil NO emission and monitored annual NO_2 flux) in subtropical forest area of South

China could compose 7.0% of national total anthropogenic emissions of NO_x, 7 Tg N yr^{-1} (Zheng et al., 2018). Nevertheless, soil emitted NO_x could be partly consumed by forest canopies, leading to certain reduction of NO_x emitted from the whole forest to atmosphere (Ganzeveld et al., 2002). Regarding the strong dependence of NO emission on soil temperature and soil moisture, higher soil NO_x emission from N-rich areas could be projected as a result of global warming (Huang et al., 2017) and prolonged drought in East Asia (Pokhrel et al., 2021) in the future. In addition, further reduction of anthropogenic NO_x emission across China has been anticipated (Xing et al., 2020) due to strict policy control and energy structure adjustment, under which soil NO_x emission from forests, grasslands and agriculture might become more and more important (Lu et al., 2021; Skiba et al., 2021), and more investigations on soil NO_x emission are required to improve air-pollution modeling.

5. Conclusions

In this study, NO and NO_2 fluxes from subtropical forest soils receiving contrasting N deposition rates were monitored at QYZ and TSP in South China for more than 6 months. WFPS and soil temperature turned to be the major impacting factors of soil NO emission at both sites, while high ambient NO concentration (>10 ppbv) at TSP induced significant NO deposition in the winter. For both sites, the optimum soil temperature was above 25 °C, while the optimum WFPS for NO release at QYZ was higher (65–70%) than that at TSP (<23%). At TSP, NO pulses were only observed after long period of drought, while NO pulses at QYZ site were observed as long as heavy rainfall occurred. Differences in soil inorganic N availability and WFPS regime between the two studied sites might cause the different responses. But the detailed mechanisms why these two subtropical forests responded differently to WFPS and rainfalls requires further investigation. The cumulative soil emissions of NO reached 0.41 ± 0.01 and 0.76 ± 0.01 kg N ha^{-1} yr^{-1} at QYZ and TSP, contributing to 2.6% and 1.7% of the annual throughfall N deposition, respectively. At both sites, NO_2 were mainly deposited to soils, accounting for 2% and 21% of soil-emitted NO at QYZ and TSP, respectively. Periodic NO_2 emissions were also observed, the complete understanding of which calls for simultaneous monitoring of NO, NO_2 and HONO fluxes in subtropical forests. Based on results in the four subtropical forests reported thus far, soil NO_x emission from overall subtropical forest area in China could accounted for 7.0% of national total anthropogenic emissions of NO_x. Considering the high spatiotemporal variability and growing importance of soil NO_x emissions, more precise estimation of soil NO_x emission from subtropical forests is needed and requires more long-term field investigations in other subtropical forests.

Author statement

Piaopiao Ke: Methodology, Investigation, Data Curation, Writing - Original Draft. **Ronghua Kang**: Conceptualization, Methodology, Investigation, Writing-Review & Editing. **Loreena Katherine Avery**: Visualization, Writing- Review & Editing. **Jiawei Zhang**: Investigation. **Qian Yu:** Methodology, Visualization. **Danni Xie**: Investigation. **Lei Duan**: Conceptualization , Writing - Review & Editing , Supervision.

Declaration of competing interest

The authors declare that they have no known competing financial interests or personal relationships that could have appeared to influence the work reported in this paper.

Acknowledgement

The authors are grateful for the financial support of the special fund of National Natural Science Foundation of China [grant number 41807320; 21607091] and State Key Joint Laboratory of Environment Simulation and Pollution Control [grant number 19L02ESPC]. The authors also greatly acknowledge the support received in monitoring system maintenance from Mingquan Zou, Bin Li and Yuanfen Huang.

Appendix A. Supplementary data

Supplementary data to this article can be found online at https://doi.org/10.1016/j.envpol.2021.118696.

Supplementary

Section S1: The correction of NO and NO_2 concentrations in the monitoring system. Table S1–S5: Seasonal averages of NO_x fluxes, ambient concentrations and metrological parameters at the two sites; Pearson's coefficient between fluxes, concentrations and metrological conditions at QYZ; Pearson's coefficients between fluxes, concentrations and metrological conditions at TSP; Pearson's coefficients between NO_2 emission, NO flux, NO concentration, NO_2 concentration and the metrological conditions; comparison of NO emission rate between this study and other ecosystems. Figure S1–S8: the flow scheme and designs of the flux chamber and base; monthly averaged fluxes without concentration corrected; variations of NO fluxes with ambient concentration; temporal variations of NO and NO_2 concentration along with solar radiation; linear regression between NO_2 flux and the concentration in different seasons; comparison between simulated and observed cumulative NO_x emission.; variations of NO flux with the N throughfall in temperate coniferous forests and subtropical forests; comparison between NO flux monitored in this study and at another previously reported coniferous subtropical forest.

References

Altshuller, A.P., Bufalini, J.J., 1971. Photochemical aspects of air pollution - review. Environ. Sci. Technol. 5, 39. https://doi.org/10.1021/es60048a001.

Bargsten, A., Falge, E., Pritsch, K., Huwe, B., Meixner, F.X., 2010. Laboratory measurements of nitric oxide release from forest soil with a thick organic layer under different understory types. Biogeosciences 7, 1425–1441. https://doi.org/10.5194/bg-7-1425-2010.

Barrat, H.A., Evans, J., Chadwick, D.R., Clark, I.M., Le Cocq, K., Cardenas, L.M., 2020. The impact of drought and rewetting on N2O emissions from soil in temperate and Mediterranean climates. Eur. J. Soil Sci. https://doi.org/10.1111/ejss.13015.

Behrendt, T., Braker, G., Song, G., Pommerenke, B., Dorsch, P., 2017. Nitric oxide emission response to soil moisture is linked to transcriptional activity of functional microbial groups. Soil Biol. Biochem. 115, 337–345. https://doi.org/10.1016/j.soilbio.2017.08.006.

Behrendt, T., Veres, P.R., Ashuri, F., Song, G., Flanz, M., Mamtimin, B., Bruse, M., Williams, J., Meixner, F.X., 2014. Characterisation of NO production and consumption: new insights by an improved laboratory dynamic chamber technique. Biogeosciences 11, 5463–5492. https://doi.org/10.5194/bg-11-5463-2014.

Butterbach-Bahl, K., Kahl, M., Mykhayliv, L., Werner, C., Kiese, R., Li, C., 2009. A European-wide inventory of soil NO emissions using the biogeochemical models DNDC/Forest-DNDC. Atmos. Environ. 43, 1392–1402. https://doi.org/10.1016/j.atmosenv.2008.02.008.

Butterbach-Bahl, K., Kock, M., Willibald, G., Hewett, B., Buhagiar, S., Papen, H., Kiese, R., 2004. Temporal variations of fluxes of NO, NO2, N2O, CO2, and CH4 in a tropical rain forest ecosystem. Global Biogeochem. Cycles 18, 11. https://doi.org/10.1029/2004gb002243.

ButterbachBahl, K., Gasche, R., Breuer, L., Papen, H., 1997. Fluxes of NO and N2O from temperate forest soils: impact of forest type, N deposition and of liming on the NO and N2O emissions. Nutrient Cycl. Agroecosyst. 48, 79–90. https://doi.org/10.1023/a:1009785521107.

Caranto, J.D., Lancaster, K.M., 2017. Nitric oxide is an obligate bacterial nitrification intermediate produced by hydroxylamine oxidoreductase. Proc. Natl. Acad. Sci. U. S. A 114, 8217–8222. https://doi.org/10.1073/pnas.1704504114.

Crutzen, P.J., 1979. Role of NO and NO2 in the chemistry of the troposphere and stratosphere. Annu. Rev. Earth Planet Sci. 7, 443–472. https://doi.org/10.1146/annurev.ea.07.050179.002303.

Davidson, E.A., Vitousek, P.M., Matson, P.A., Riley, R., Garciamendez, G., Maass, J.M., 1991. Soil emissions of nitric-oxide in a seasonally dry tropical forest of Mexico. J. Geophys. Res. Atmos. 96, 15439–15445. https://doi.org/10.1029/91jd01476.

Delon, C., Galy-Lacaux, C., Serca, D., Loubet, B., Camara, N., Gardrat, E., Saneh, I., Fensholt, R., Tagesson, T., Le Dantec, V., Sambou, B., Diop, C., Mougin, E., 2017. Soil and vegetation-atmosphere exchange of NO, NH3, and N2O from field measurements in a semi arid grazed ecosystem in Senegal. Atmos. Environ. 156, 36–51. https://doi.org/10.1016/j.atmosenv.2017.02.024.

Fang, S., Mu, Y., 2009. NOX fluxes from several typical agricultural fields during summer-autumn in the Yangtze Delta, China. Atmos. Environ. 43, 2665–2671. https://doi.org/10.1016/j.atmosenv.2009.02.027.
FAO, 2020. Global Forest Resources Assessment 2020.
Firestone, M., Davidson, E., 1989. Microbiological basis of NO and N2O production and consumption in soil. In: Exchange of Trace Gases between Terrestrial Ecosystems and the Atmosphere, vol. 47. John Wiley & Sons, Ltd, pp. 7–21.
Galloway, J.N., Dentener, F.J., Capone, D.G., Boyer, E.W., Howarth, R.W., Seitzinger, S. P., Asner, G.P., Cleveland, C.C., Green, P.A., Holland, E.A., Karl, D.M., Michaels, A. F., Porter, J.H., Townsend, A.R., Vöosmarty, C.J., 2004. Nitrogen cycles: past, present, and future. Biogeochemistry 70, 153–226. https://doi.org/10.1007/s10533-004-0370-0.
Ganzeveld, L.N., Lelieveld, J., Dentener, F.J., Krol, M.C., Bouwman, A.J., Roelofs, G.J., 2002. Global soil-biogenic NOx emissions and the role of canopy processes. J. Geophys. Res. Atmos. 107 https://doi.org/10.1029/2001jd001289. ACH 9.
Goldberg, S.D., Gebauer, G., 2009. N2O and NO fluxes between a Norway spruce forest soil and atmosphere as affected by prolonged summer drought. Soil Biol. Biochem. 41, 1986–1995. https://doi.org/10.1016/j.soilbio.2009.07.001.
Gut, A., Scheibe, M., Rottenberger, S., Rummel, U., Welling, M., Ammann, C., Kirkman, G.A., Kuhn, U., Meixner, F.X., Kesselmeier, J., Lehmann, B.E., Schmidt, W., Muller, E., Piedade, M.T.F., 2002. Exchange fluxes of NO2 and O-3 at soil and leaf surfaces in an Amazonian rain forest. J. Geophys. Res. Atmos. 107, D20 https://doi.org/10.1029/2001jd000654.
Hassler, E., Corre, M.D., Kurniawan, S., Veldkamp, E., 2017. Soil nitrogen oxide fluxes from lowland forests converted to smallholder rubber and oil palm plantations in Sumatra, Indonesia. Biogeosciences 14, 2781–2798. https://doi.org/10.5194/bg-14-2781-2017.
Heil, J., Vereecken, H., Brueggemann, N., 2016. A review of chemical reactions of nitrification intermediates and their role in nitrogen cycling and nitrogen trace gas formation in soil. Eur. J. Soil Sci. 67, 23–39. https://doi.org/10.1111/ejss.12306.
Holland, E.A., Dentener, F.J., Braswell, B.H., Sulzman, J.M., 1999. Contemporary and pre-industrial global reactive nitrogen budgets. Biogeochemistry 46, 7–43. https://doi.org/10.1007/bf01007572.
Homyak, P.M., Blankinship, J.C., Marchus, K., Lucero, D.M., Sickman, J.O., Schimel, J.P., 2016. Aridity and plant uptake interact to make dryland soils hotspots for nitric oxide (NO) emissions. Proc. Natl. Acad. Sci. U. S. A 113, E2608–E2616. https://doi.org/10.1073/pnas.1520496113.
Homyak, P.M., Kamiyama, M., Sickman, J.O., Schimel, J.P., 2017. Acidity and organic matter promote abiotic nitric oxide production in drying soils. Global Change Biol. 23, 1735–1747. https://doi.org/10.1111/gcb.13507.
Huang, J., Yu, H., Dai, A., Wei, Y., Kang, L., 2017. Drylands face potential threat under 2 degrees C global warming target. Nat. Clim. Change 7, 417. https://doi.org/10.1038/nclimate3275.
Huang, Y., Kang, R., Mulder, J., Zhang, T., Duan, L., 2015. Nitrogen saturation, soil acidification, and ecological effects in a subtropical pine forest on acid soil in southwest China. J. Geophys. Res. Biogeosci. 120, 2457–2472. https://doi.org/10.1002/2015jg003048.
Huang, Y., Li, D.J., 2014. Soil nitric oxide emissions from terrestrial ecosystems in China: a synthesis of modeling and measurements. Sci. Rep. 4, 8. https://doi.org/10.1038/srep07406.
Hudman, R.C., Moore, N.E., Mebust, A.K., Martin, R.V., Russell, A.R., Valin, L.C., Cohen, R.C., 2012. Steps towards a mechanistic model of global soil nitric oxide emissions: implementation and space based-constraints. Atmos. Chem. Phys. 12, 7779–7795. https://doi.org/10.5194/acp-12-7779-2012.
Kang, R., Yu, L., Dorsch, P., Mulder, J., 2019. Nitrification is the primary source for NO in N-saturated subtropical forest soils: results from in-situ 15 N labeling. Rapid Communications in Mass Spectrometry. RCM. https://doi.org/10.1002/rcm.8700 e8700-e8700.
Kang, R.H., Mulder, J., Duan, L., Dorsch, P., 2017. Spatial and temporal variability of soil nitric oxide emissions in N-saturated subtropical forest. Biogeochemistry 134, 337–351. https://doi.org/10.1007/s10533-017-0368-z.
Ke, P., Yu, Q., Luo, Y., Kang, R., Duan, L., 2020. Fluxes of nitrogen oxides above a subtropical forest canopy in China. Sci. Total Environ. 715, 136993. https://doi.org/10.1016/j.scitotenv.2020.136993.
Kleffmann, J., Tapia, G.V., Bejan, I., Kurtenbach, R., Wiesen, P., 2013. NO2 measurement techniques: pitfalls and new developments. In: Barnes, I., Rudziński, K.J. (Eds.), Disposal of Dangerous Chemicals in Urban Areas and Mega Cities. Springer Netherlands, Dordrecht, pp. 15–28.
Leitner, S., Homyak, P.M., Blankinship, J.C., Eberwein, J., Jenerette, G.D., Zechmeister-Boltenstern, S., Schimel, J.P., 2017. Linking NO and N2O emission pulses with the mobilization of mineral and organic N upon rewetting dry soils. Soil Biol. Biochem. 115, 461–466. https://doi.org/10.1016/j.soilbio.2017.09.005.
Li, D., Wang, X., Mo, J., Sheng, G., Fu, J., 2007. Soil nitric oxide emissions from two subtropical humid forests in south China. J. Geophys. Res. Atmos. 112, D23302 https://doi.org/10.1029/2007jd008680.
Li, X., Brauers, T., Haeseler, R., Bohn, B., Fuchs, H., Hofzumahaus, A., Holland, F., Lou, S., Lu, K.D., Rohrer, F., Hu, M., Zeng, L.M., Zhang, Y.H., Garland, R.M., Su, H., Nowak, A., Wiedensohler, A., Takegawa, N., Shao, M., Wahner, A., 2012. Exploring the atmospheric chemistry of nitrous acid (HONO) at a rural site in Southern China. Atmos. Chem. Phys. 12, 1497–1513. https://doi.org/10.5194/acp-12-1497-2012.
Li, Y., Pang, J., Peng, C., Zhang, S., Hou, L., Chen, S., Wang, X., Zhang, H., 2017. NO flux in forest soil at different elevation of Huoditang area in the Qinling mountains. J. Northeast For. Univ. 45, 42–49.
Liu, S.W., Lin, F., Wu, S., Ji, C., Sun, Y., Jin, Y.G., Li, S.Q., Li, Z.F., Zou, J.W., 2017. A meta-analysis of fertilizer-induced soil NO and combined NO+N2O emissions. Global Change Biol. 23, 2520–2532. https://doi.org/10.1111/gcb.13485.
Lu, X., Ye, X., Zhou, M., Zhao, Y., Weng, H., Kong, H., Li, K., Gao, M., Zheng, B., Lin, J., Zhou, F., Zhang, Q., Wu, D., Zhang, L., Zhang, Y., 2021. The underappreciated role of agricultural soil nitrogen oxide emissions in ozone pollution regulation in North China. Nat. Commun. 12, 5021. https://doi.org/10.1038/s41467-021-25147-9, 5021.
Luo, G.J., Brueggemann, N., Wolf, B., Gasche, R., Grote, R., Butterbach-Bahl, K., 2012. Decadal variability of soil CO2, NO, N2O, and CH4 fluxes at the Hoglwald Forest, Germany. Biogeosciences 9, 1741–1763. https://doi.org/10.5194/bg-9-1741-2012.
Mayer, J.C., Bargsten, A., Rummel, U., Meixner, F.X., Foken, T., 2011. Distributed Modified Bowen Ratio method for surface layer fluxes of reactive and non-reactive trace gases. Agric. For. Meteorol. 151, 655–668. https://doi.org/10.1016/j.agrformet.2010.10.001.
Medinets, S., Gasche, R., Kiese, R., Rennenberg, H., Butterbach-Bahl, K., 2019. Seasonal dynamics and profiles of soil NO concentrations in a temperate forest. Plant Soil 445, 335–348. https://doi.org/10.1007/s11104-019-04305-5.
Medinets, S., Gasche, R., Skiba, U., Medinets, V., Butterbach-Bahl, K., 2016a. The impact of management and climate on soil nitric oxide fluxes from arable land in the Southern Ukraine. Atmos. Environ. 137, 113–126. https://doi.org/10.1016/j.atmosenv.2016.04.032.
Medinets, S., Gasche, R., Skiba, U., Schindlbacher, A., Kiese, R., Butterbach-Bahl, K., 2016b. Cold season soil NO fluxes from a temperate forest: drivers and contribution to annual budgets. Environ. Res. Lett. 11, 11. https://doi.org/10.1088/1748-9326/11/11/114012.
Medinets, S., Skiba, U., Rennenberg, H., Butterbach-Bahl, K., 2015. A review of soil NO transformation: associated processes and possible physiological significance on organisms. Soil Biol. Biochem. 80, 92–117. https://doi.org/10.1016/j.soilbio.2014.09.025.
Medinets, S., White, S., Cowan, N., Drewer, J., Dick, J., Jones, M., Andrews, C., Harvey, D., Skiba, U., 2021. Impact of climate change on soil nitric oxide and nitrous oxide emissions from typical land uses in Scotland. Environ. Res. Lett. 16, 055035 https://doi.org/10.1088/1748-9326/abf06e.
Molina-Herrera, S., Haas, E., Grote, R., Kiese, R., Klatt, S., Kraus, D., Kampffmeyer, T., Friedrich, R., Andreae, H., Loubet, B., Ammann, C., Horvath, L., Larsen, K., Gruening, C., Frumau, A., Butterbach-Bahl, K., 2017. Importance of soil NO emissions for the total atmospheric NOX budget of Saxony, Germany. Atmos. Environ. 152, 61–76. https://doi.org/10.1016/j.atmosenv.2016.12.022.
Mushinski, R.M., Payne, Z.C., Raff, J.D., Craig, M.E., Pusede, S.E., Rusch, D.B., White, J. R., Phillips, R.P., 2021. Nitrogen cycling microbiomes are structured by plant mycorrhizal associations with consequences for nitrogen oxide fluxes in forests. Global Change Biol. 27, 1068–1082. https://doi.org/10.1111/gcb.15439.
Mushinski, R.M., Phillips, R.P., Payne, Z.C., Abney, R.B., Jo, I., Fei, S.L., Pusede, S.E., White, J.R., Rusch, D.B., Raff, J.D., 2019. Microbial mechanisms and ecosystem flux estimation for aerobic NOy emissions from deciduous forest soils. Proc. Natl. Acad. Sci. U. S. A 116, 2138–2145. https://doi.org/10.1073/pnas.1814632116.
Pacifico, F., Delon, C., Jambert, C., Durand, P., Morris, E., Evans, M.J., Lohou, F., Derrien, S., Donnou, V.H.E., Houeto, A.V., Martinez, I.R., Brilouet, P.E., 2019. Measurements of nitric oxide and ammonia soil fluxes from a wet savanna ecosystem site in West Africa during the DACCIWA field campaign. Atmos. Chem. Phys. 19, 2299–2325. https://doi.org/10.5194/acp-19-2299-2019.
Perez, I.M., Wooldridge, P.J., Cohen, R.C., 2007. Laboratory evaluation of a novel thermal dissociation chemiluminescence method for in situ detection of nitrous acid. Atmos. Environ. 41, 3993–4001. https://doi.org/10.1016/j.atmosenv.2007.01.060.
Pilegaard, K., 2013. Processes regulating nitric oxide emissions from soils. Philos. Trans. R. Soc. Lond. B Biol. Sci. 368.
Pilegaard, K., Skiba, U., Ambus, P., Beier, C., Brueggemann, N., Butterbach-Bahl, K., Dick, J., Dorsey, J., Duyzer, J., Gallagher, M., Gasche, R., Horvath, L., Kitzler, B., Leip, A., Pihlatie, M.K., Rosenkranz, P., Seufert, G., Vesala, T., Westrate, H., Zechmeister-Boltenstern, S., 2006. Factors controlling regional differences in forest soil emission of nitrogen oxides (NO and N2O). Biogeosciences 3, 651–661.
Pokhrel, Y., Felfelani, F., Satoh, Y., Boulange, J., Burek, P., Gaedeke, A., Gerten, D., Gosling, S.N., Grillakis, M., Gudmundsson, L., Hanasaki, N., Kim, H., Koutroulis, A., Liu, J., Papadimitriou, L., Schewe, J., Mueller Schmied, H., Stacke, T., Telteu, C.-E., Thiery, W., Veldkamp, T., Zhao, F., Wada, Y., 2021. Global terrestrial water storage and drought severity under climate change. Nat. Clim. Change 11, 226–233. https://doi.org/10.1038/s41558-020-00972-w.
Recio, J., Alvarez, J.M., Rodriguez-Quijano, M., Vallejo, A., 2019. Nitrification inhibitor DMPSA mitigated N2O emission and promoted NO sink in rainfed wheat. Environ. Pollut. 245, 199–207.doi. https://doi.org/10.1016/j.envpol.2018.10.135.
Recio, J., Montoya, M., Álvarez, J.M., Vallejo, A., 2020. Inhibitor-coated enhanced-efficiency N fertilizers for mitigating NOx and N2O emissions in a high-temperature irrigated agroecosystem. Agric. For. Meteorol. 292–293, 108110. https://doi.org/10.1016/j.agrformet.2020.108110.
Schindlbacher, A., Zechmeister-Boltenstern, S., Butterbach-Bahl, K., 2004. Effects of soil moisture and temperature on NO, NO2, and N2O emissions from European forest soils. J. Geophys. Res. Atmos. 109, D17302 https://doi.org/10.1029/2004JD004590.
Schwede, D.B., Simpson, D., Tan, J., Fu, J.S., Dentener, F., Du, E., deVries, W., 2018. Spatial variation of modelled total, dry and wet nitrogen deposition to forests at global scale. Environ. Pollut. 243, 1287–1301. https://doi.org/10.1016/j.envpol.2018.09.084.
Seinfeld, J.H., Pandis, S.N., 2012. Atmospheric Chemistry and Physics: from Air Pollution to Climate Change, second ed. John Wiley & Sons, New York.
Skiba, U., Medinets, S., Cardenas, L.M., Carnell, E.J., Hutchings, N., Amon, B., 2021. Assessing the contribution of soil NOx emissions to European atmospheric pollution. Environ. Res. Lett. 16 https://doi.org/10.1088/1748-9326/abd2f2.

Song, L., Drewer, J., Zhu, B., Zhou, M., Cowan, N., Levy, P., Skiba, U., 2020. The impact of atmospheric N deposition and N fertilizer type on soil nitric oxide and nitrous oxide fluxes from agricultural and forest Eutric Regosols. Biol. Fertil. Soils 56, 1077–1090. https://doi.org/10.1007/s00374-020-01485-6.

Sørbotten, L., 2011. Hill Slope Unsaturated Flowpaths and Soil Moisture Variability in a Forested Catchment in Southwest China. Institute of Plant and Environmental Sciences, Norwegian University of Life Science (Master thesis).

Sörgel, M., Trebs, I., Wu, D., Held, A., 2015. A comparison of measured HONO uptake and release with calculated source strengths in a heterogeneous forest environment. Atmos. Chem. Phys. 15, 9237–9251. https://doi.org/10.5194/acp-15-9237-2015.

Tang, K., Qin, M., Fang, W., Duan, J., Meng, F., Ye, K., Zhang, H., Xie, P., Liu, J., Liu, W., Feng, Y., Huang, Y., Ni, T., 2020. An automated dynamic chamber system for exchange flux measurement of reactive nitrogen oxides (HONO and NOx) in farmland ecosystems of the Huaihe River Basin, China. Sci. Total Environ. 745, 140867. https://doi.org/10.1016/j.scitotenv.2020.140867.

Tian, J., Dungait, J.A.J., Lu, X., Yang, Y., Hartley, I.P., Zhang, W., Mo, J., Yu, G., Zhou, J., Kuzyakov, Y., 2019. Long-term nitrogen addition modifies microbial composition and functions for slow carbon cycling and increased sequestration in tropical forest soil. Global Change Biol. 25, 3267–3281. https://doi.org/10.1111/gcb.14750.

Udert, K.M., Larsen, T.A., Gujer, W., 2005. Chemical nitrite oxidation in acid solutions as a consequence of microbial ammonium oxidation. Environ. Sci. Technol. 39, 4066–4075. https://doi.org/10.1021/es048422m.

Wang, J., Li, Q., Fu, X., Dai, X., Kou, L., Xu, M., Chen, S., Chen, F., Wang, H., 2019. Mechanisms driving ecosystem carbon sequestration in a Chinese fir plantation: nitrogen versus phosphorus fertilization. Eur. J. For. Res. 138, 863–873. https://doi.org/10.1007/s10342-019-01208-z.

Wang, W., Shi, Z., Luo, D., Liu, S., Lu, L., 2013. Characteristics of soil microbial biomass and community composition in three types of plantations in southern subtropical area of China. Yingyong Shengtai Xuebao 24, 1784–1792.

Wang, Y., Wang, H., Xu, M., Ma, Z., Wang, Z.-L., 2015. Soil organic carbon stocks and CO2 effluxes of native and exotic pine plantations in subtropical China. Catena 128, 167–173. https://doi.org/10.1016/j.catena.2015.02.003.

Wen, X.F., Wang, H.M., Wang, J.L., Yu, G.R., Sun, X.M., 2010. Ecosystem carbon exchanges of a subtropical evergreen Coniferous plantation subjected to seasonal drought. Biogeosciences 7, 357–369, 2003–2007.

Weng, H., Lin, J., Martin, R., Millet, D.B., Jaegle, L., Ridley, D., Keller, C., Li, C., Du, M., Meng, J., 2020. Global high-resolution emissions of soil NOx, sea salt aerosols, and biogenic volatile organic compounds. Sci. Data 7, 148. https://doi.org/10.1038/s41597-020-0488-5.

Wu, D., Horn, M.A., Behrendt, T., Müller, S., Li, J., Cole, J.A., Xie, B., Ju, X., Li, G., Ermel, M., Oswald, R., Fröhlich-Nowoisky, J., Hoor, P., Hu, C., Liu, M., Andreae, M. O., Pöschl, U., Cheng, Y., Su, H., Trebs, I., Weber, B., Sörgel, M., 2019. Soil HONO emissions at high moisture content are driven by microbial nitrate reduction to nitrite: tackling the HONO puzzle. ISME J. 13, 1688–1699. https://doi.org/10.1038/s41396-019-0379-y.

Wu, X., Brüggemann, N., Gasche, R., Shen, Z., Wolf, B., Butterbach-Bahl, K., 2010. Environmental controls over soil-atmosphere exchange of N2O, NO, and CO2 in a temperate Norway spruce forest. Global Biogeochem. Cycles 24, GB2012. https://doi.org/10.1029/2009GB003616.

Xie, D.N., 2020. Response of Soil and Surface Water Chemistry in Subtropical Forests to Decreasing Nitrogen Deposition. School of Environment, Tsinghua University (Ph.D. Thesis).

Xing, J., Lu, X., Wang, S., Wang, T., Ding, D., Yu, S., Shindell, D., Ou, Y., Morawska, L., Li, S., Ren, L., Zhang, Y., Loughlin, D., Zheng, H., Zhao, B., Liu, S., Smith, K.R., Hao, J., 2020. The quest for improved air quality may push China to continue its CO2 reduction beyond the Paris Commitment. Proc. Natl. Acad. Sci. U. S. A 117, 29535–29542. https://doi.org/10.1073/pnas.2013297117.

Xu, S.G., Liu, Y.F., Cui, Y.G., Pei, Z.Y., 2011. Litter decomposition in a subtropical plantation in Qianyanzhou, China. J. For. Res. 16, 8–15. https://doi.org/10.1007/s10310-010-0206-9.

Yu, J.B., Meixner, F.X., Sun, W.D., Liang, Z.W., Chen, Y., Mamtimin, B., Wang, G.P., Sun, Z.G., 2008. Biogenic nitric oxide emission from saline sodic soils in a semiarid region, northeastern China: a laboratory study. J. Geophys. Res.: Biogeosciences 113, G04005. https://doi.org/10.1029/2007JG000576.

Yu, J.B., Meixner, F.X., Sun, W.D., Mamtimin, B., Xia, C.H., Xie, W.J., 2010. Biogenic nitric oxide emission of mountain soils sampled from different vertical landscape zones in the Changbai mountains, northeastern China. Environ. Sci. Technol. 44, 4122–4128. https://doi.org/10.1021/es100380m.

Yu, Q., Duan, L., Yu, L., Chen, X., Si, G., Ke, P., Ye, Z., Mulder, J., 2018. Threshold and multiple indicators for nitrogen saturation in subtropical forests. Environ. Pollut. 241, 664–673. https://doi.org/10.1016/j.envpol.2018.06.001.

Zheng, B., Tong, D., Li, M., Liu, F., Hong, C.P., Geng, G.N., Li, H.Y., Li, X., Peng, L.Q., Qi, J., Yan, L., Zhang, Y.X., Zhao, H.Y., Zheng, Y.X., He, K.B., Zhang, Q., 2018. Trends in China's anthropogenic emissions since 2010 as the consequence of clean air actions. Atmos. Chem. Phys. 18, 14095–14111. https://doi.org/10.5194/acp-18-14095-2018.

Zhu, J., Mulder, J., Solheimslid, S.O., Dörsch, P., 2013. Functional traits of denitrification in a subtropical forest catchment in China with high atmogenic N deposition. Soil Biol. Biochem. 57, 577–586. https://doi.org/10.1016/j.soilbio.2012.09.017.